INFORMATION TO USERS

This manuscript has been reproduced from the microfilm master. UMI films the text directly from the original or copy submitted. Thus, some thesis and dissertation copies are in typewriter face, while others may be from any type of computer printer.

The quality of this reproduction is dependent upon the quality of the copy submitted. Broken or indistinct print, colored or poor quality illustrations and photographs, print bleedthrough, substandard margins, and improper alignment can adversely affect reproduction.

In the unlikely event that the author did not send UMI a complete manuscript and there are missing pages, these will be noted. Also, if unauthorized copyright material had to be removed, a note will indicate the deletion.

Oversize materials (e.g., maps, drawings, charts) are reproduced by sectioning the original, beginning at the upper left-hand corner and continuing from left to right in equal sections with small overlaps.

Photographs included in the original manuscript have been reproduced xerographically in this copy. Higher quality 6" x 9" black and white photographic prints are available for any photographs or illustrations appearing in this copy for an additional charge. Contact UMI directly to order.

ProQuest Information and Learning
300 North Zeeb Road, Ann Arbor, MI 48106-1346 USA
800-521-0600

CRATER FEATURES DIAGNOSTIC OF OBLIQUE IMPACTS: THE SIZE AND POSITION OF THE CENTRAL PEAK

by

Andreas Gunnar Ekholm

A Thesis Submitted to the Faculty of the

DEPARTMENT OF PLANETARY SCIENCES

In Partial Fulfillment of the Requirements
For the Degree of

MASTER OF SCIENCE

In the Graduate College

THE UNIVERSITY OF ARIZONA

2001

UMI Number: 1407000

Bell & Howell Information and Learning Company
300 North Zeeb Road
P.O. Box 1346
Ann Arbor, MI 48106-1346

STATEMENT BY AUTHOR

This thesis has been submitted in partial fulfillment of requirements for an advanced degree at The University of Arizona and is deposited in the University Library to be made available to borrowers under the rules of the Library.

Brief quotations from this thesis are allowable without special permission, provided that accurate acknowledgment of the source is made. Requests for permission for extended quotation from or reproduction of this manuscript in whole or in part may be granted by the head of the major department or the Dean of the Graduate College when in his or her judgment the proposed use of the material is in the interests of scholarship. In all other instances, however, permission must be obtained from the author.

SIGNED: Andrew Ekholm

APPROVAL BY THESIS DIRECTOR

This thesis has been approved on the date shown below:

H. Jay Melosh
Professor of Planetary Sciences

10/31/01
Date

ACKNOWLEDGMENTS

I would like to thank my advisor, Jay Melosh, for his support through good times as well as bad. I would also like to thank Bob Strom for providing me with the central peak diameters, as well as for many productive discussions.

TABLE OF CONTENTS

LIST OF FIGURES

LIST OF TABLES

ABSTRACT

Using Magellan data, I have investigated two crater characteristics that have been cited as diagnostic of oblique impacts: an uprange offset of the central peak in complex craters, and an increasing central peak diameter relative to crater diameter with decreasing impact angle. I find that the offset distribution is random and very similar to that for high-angle impacts, and that there is no correlation between central peak diameter and impact angle. Accordingly, these two crater characteristics cannot be used to infer the impact angle or direction.

CHAPTER 1

Introduction

1.1. General background

Impact cratering is the most prevalent geologic process in the solar system, and the only one to affect all solid planetary bodies. Impact craters come in all sizes; from the micrometer-sized craters seen in lunar rocks brought back by the Apollo astronauts, to the gargantuan 2000 km diameter Hellas basin on Mars. They are classified into three main categories depending on their morphological appearance, which correlates with their diameter: simple craters (smallest), complex craters, and multiring basins (largest). The classic crater type, simple craters, are bowl-shaped depressions with a raised rim, surrounded by an ejecta blanket of material thrown out of the crater during its excavation. Complex craters have terraced walls and flat floors, with a central peak or peak ring at the center, and are believed to form by collapse of an initially bowl-shaped transient crater. The very largest impact structures, multiring basins, are surrounded by multiple concentric circular scarps, hence the name.

The transition diameters between the different classes depend on gravity and thus vary from planet to planet; for the Earth, the transition between simple and complex craters occurs at a diameter of 3–6 km, for the moon, at about 15 km. The transition diameter between complex craters and multiring basins is not a simple function of gravity and not well defined.

1.2. Oblique impacts

The most probable impact angle for planetary impacts is 45° (Gilbert, 1893; Shoemaker, 1962). Hence, when studying a crater, one cannot assume that the impact was close to vertical, and criteria are needed by which to judge the degree of obliquity, as well as the impact direction. A number of such criteria have been proposed; the two most prominent are a missing wedge-shaped sector in the uprange ejecta (i.e. the part of the ejecta deposits lying in the direction from which the impactor came), and a depressed uprange rim (for impact angles less than about 10° the downrange rim is also depressed). These two, as well as a steeper slope of the uprange crater wall relative to the downrange wall, and an elliptical shape for very shallow impact angles (<10°), were derived from laboratory scale experiments by Gault and Wedekind (1978). The existence of these features—albeit not their dependence on impact angle—has been verified observationally (see e.g. Herrick and Forsberg, 1998; Forsberg et al., 1998), and they are thus considered safe indicators of oblique impacts (however, the slope difference might not exist for complex craters; see Section 4.1).

Additional criteria for oblique impacts that have been derived from observations of planetary scale impacts include: (1) an uprange offset of the central uplift (i.e., peak or peak ring) in complex craters (Schultz, 1992a,b), (2) an increasing central uplift diameter relative to crater diameter with decreasing impact angle (Schultz, 1992a,b), (3) a breach in the central peak complex parallel to the trajectory (Schultz and Anderson, 1996), and (4) a smaller depth/diameter ratio than normal for small craters on bodies with a dense

atmosphere, probably due to atmospheric breakup of the impactor (Schultz and Anderson, 1996; Herrick and Forsberg, 1998).

Observations (1) and (2) have most frequently been put to use in studies of terrestrial craters, as the most prominent obliquity indicators described above (the shape of the ejecta deposits and the variation in rim height) have almost always been obscured or removed by erosion and/or burial. (1) and (2) are much more widely applicable in that they only require that the outline of the crater and the central peak be determined. The best known crater to which one of these criteria has been applied is Chicxulub, for which both Schultz and D'Hondt (1996) and Hildebrand et al. (1998) have used (1) to infer the direction of approach and impact angle of the bolide.

With this in mind, I felt it was important to test (1) and (2) with a more extensive data set than originally employed by Schultz (1992a,b). To this end, I have conducted a systematic study of central peak (but not peak ring) sizes and positions in Venusian complex craters formed by oblique impacts, the results of which are presented in this thesis.

CHAPTER 2

Data Analysis

2.1. Measurement techniques

The position of the central peak relative to the center of the crater was determined by manually fitting ellipses to the crater rim and the base of the central peak (defining the positions of the crater center and the central peak as equal to the respective centers of these ellipses). Significant outliers to the central peak were included as part of the peak if close to the main peak, but were neglected if few in number (2–3) and well separated from the main peak. Craters with highly fragmented peaks were removed from the sample.

The direction of impact for a crater was determined as the direction in which the missing wedge-shaped sector in the uprange ejecta pointed (as defined by the centerline through the wedge), and the angle of impact was determined from the shape of the wedge (see appendix for details). The central peak diameters were taken from unpublished work by R. G. Strom. Strom's peak diameters were used because his sample was larger and his measurements more accurate; he calculated effective diameters by measuring the areas of the peaks.

2.2. Error estimates and assumptions

An average measurement error of the offsets was estimated by re-measuring 60% of the craters. This is admittedly a crude method, but I found that it produced a reasonable

error estimate. The error in Strom's central peak diameters was similarly assessed by comparing my measurements with his.

I chose Venusian craters for this study because they are mostly pristine, with undisturbed ejecta deposits, which is the key to recognizing oblique impacts and determining the impact angle. But a potentially serious problem with the Magellan data set is that topographic features are distorted in radar images in the range direction (perpendicular to the orbital track; Ford et al., 1993). To fully correct for these distortions, topographical information in the form of high-resolution altimetry data or stereo imagery is required. However, matters are simplified greatly if one makes the assumption that the rim heights and wall slopes along a range profile through the center of the crater are equal. This is equivalent to assuming that the edge of the crater floor is equidistant from the rim on these two sides of the crater, or that the range position of the central peak relative to the center of the crater is equal to its position relative to the center of the floor. Thus, under the additional assumption that the edge of the floor is level with the base of the central peak (so that there are no topography-induced distortions of their relative positions), the necessary correction reduces to measuring the range component of the central peak offset relative to the center of the crater floor instead of the center of the ellipse described by the rim.

The above assumption would obviously be valid for a symmetric crater resulting from a near-vertical impact, but will inevitably introduce errors when applied to an oblique impact crater (remember the depressed uprange rim and possibly steeper wall slope). This "approximation error" varies greatly depending on the impact direction relative to the

radar orbital track, being largest when they are perpendicular, and smallest when they are parallel. As the impact direction is random, the error will be random and not systematic. I obtained a rough estimate of the average error by making stereo measurements of a few craters, and added this to the measurement error determined as described above. The measurement error makes up 60%, and the approximation error 40%, of the total error cited in Chapter 3. This is likely to be a conservative estimate, as the average offset for craters with impact directions close to parallel with the orbital track was statistically indistinguishable from that for the full sample.

2.3. Crater sample

In selecting the sample of craters to be studied, I used the USGS/University of Arizona Venus Crater Database. The craters used ranged from 15.5 to 70.4 km in diameter, with most craters being between 20 and 40 km in size. The craters were selected according to the following criteria: (1) prominent, asymmetric ejecta deposits, (2) easily identifiable rim, and (3) clearly defined outline of the central peak. The last criterion caused my sample to contain very few bright-floored craters. It has been suggested that bright-floored craters are younger than dark-floored craters, and that the floors of dark-floored craters have been flooded by lava subsequent to formation (e.g. Izenberg et al., 1994; Wichman, 1999; Herrick and Sharpton, 2000). The possible effects of such flooding on my results will be considered in Section 4.2.

CHAPTER 3

Results

Fig. 1 shows the central peak offsets measured for 60 Venusian oblique impact craters (listed in Table 1). The impact direction is from left to right (i.e. 0° is downrange, 180° is uprange) and all the offsets have been normalized to the crater diameter. The distribution is approximately gaussian, suggesting it is random, and the offsets are all small—the average length of the offset vectors is only 0.031 crater diameters. The one-sigma average error for the individual offsets is 0.015 crater diameters both along (0°) and across (90°) the trajectory. The average offset is 0.009 straight uprange (±0.002 along and across the trajectory). The qualitative appearance of the offset distribution does not change appreciably with impact angle or crater size.

For comparison, Fig. 2 shows the central peak offsets for 25 high-angle impact craters (listed in Table 2). These were selected according to the same criteria as listed above for oblique impact craters, with the exception that the ejecta deposits are symmetric instead of asymmetric. As expected, the offsets are randomly distributed. The spread is slightly smaller (the average length of the offset vectors is 0.024 crater diameters) and the average offset slightly larger and not straight uprange (0.010 at 116°, ±0.003), but there are no significant differences.

It is obvious from Fig. 1 that one cannot draw any conclusions about the impact direction for an individual crater by measuring the offset of its central peak. But as the average offset is significantly different from zero, and straight uprange, one might

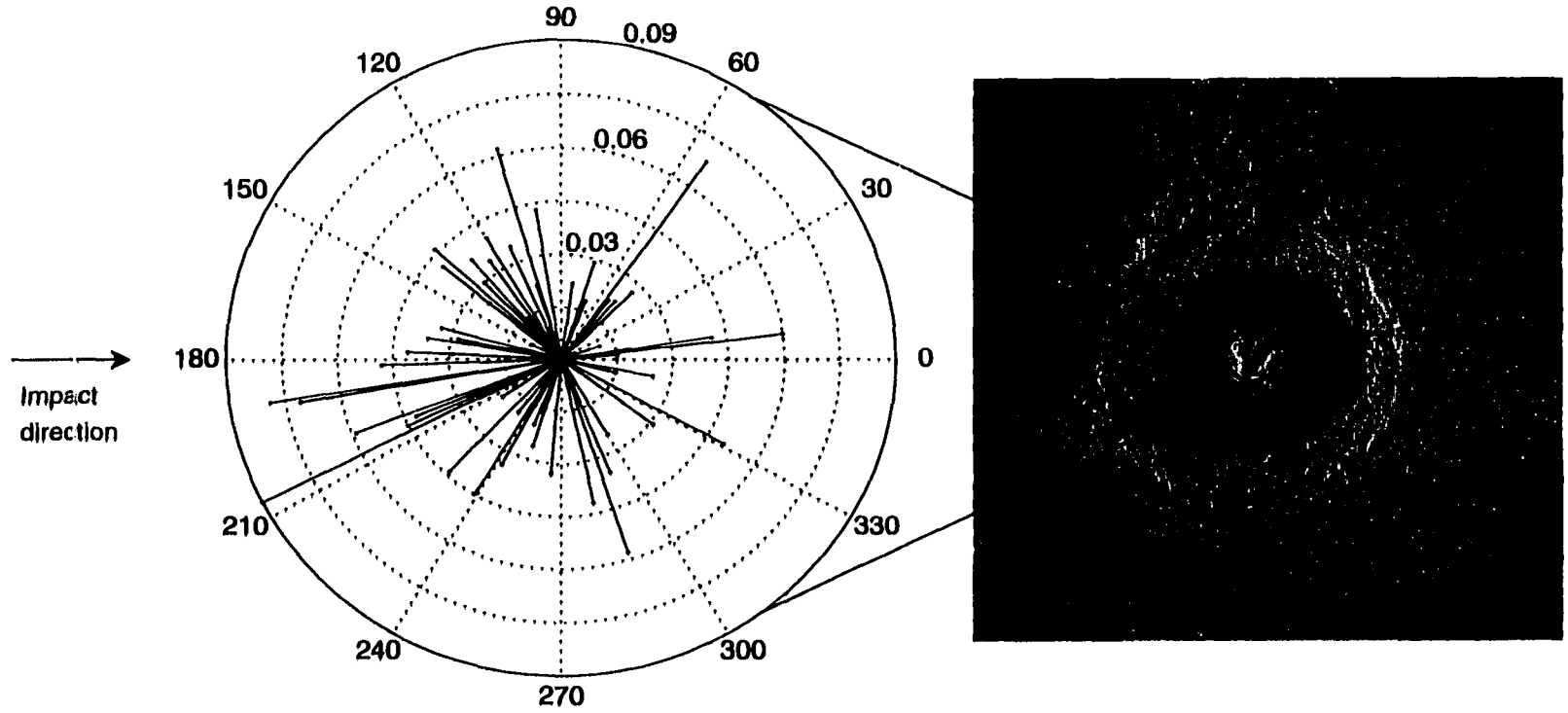

FIGURE 1: Central peak offsets measured for 60 Venusian oblique impact craters, with an example crater (29.1 km in diameter, offset 0.017 at -99° from the impact direction) for scale. The impact direction is from left to right, and all the offsets have been normalized to the crater diameter. The one-sigma average error for the individual offsets is 0.015 crater diameters both along (0°) and across (90°) the impact trajectory. The average offset is 0.009 straight uprange (±0.002 along and across the trajectory).

TABLE 1: Data for oblique impact craters. d is the crater diameter in km, A_{min} and A_{max} the lower and upper limits, respectively, of the range of possible impact angle classes, d_{cp} the central peak diameter as a fraction of the crater diameter, r the central peak offset magnitude as a fraction of the crater diameter, and θ the central peak offset angle in degrees counter-clockwise from the downrange direction.

TABLE 1: Data for oblique impact craters

Lat. (°N)	Long. (°E)	d	A_{min}	A_{max}	d_{cp}	r	θ
38.7	292.2	15.5	2	3	0.280	0.000	15
32.9	336.1	19.0	2.5	3.5	0.355	0.021	202
40.1	331.5	19.4	3.5	4	0.206	0.046	137
17.9	102.6	19.8	3	4	0.355	0.025	140
14.5	166.6	20.1	3	3	0.240	0.034	124
-6.5	275.6	20.7	3	3.5	0.204	0.011	20
-60.1	145.7	20.8	2	4.5	0.213	0.058	288
-34.3	238.9	21.6	3.5	3.5	0.266	0.008	5
-47.8	277.7	21.7	1	1		0.029	72
4.7	193.5	21.8	3	3	0.279	0.030	133
15.3	4.0	22.9	7	7	0.240	0.043	99
3.4	233.9	22.9	7	7	0.249	0.000	334
5.9	125.1	22.9	7	7	0.229	0.020	249
45.3	283.1	22.9	1	1		0.025	300
13.2	217.8	23.4	3	3	0.301	0.015	345
28.3	4.9	23.4	6	6	0.258	0.062	106
8.0	244.5	23.4	4	5	0.145	0.022	49
43.9	359.9	23.6	1	1	0.248	0.031	323
29.5	0.5	24.5	3	3.5	0.299	0.019	214
46.4	144.1	24.6	1	2.5	0.238	0.015	5
-50.5	93.3	25.2	4	4	0.229	0.037	130
-13.0	272.5	25.2	3.5	4		0.050	331
49.4	27.1	25.5	3	3		0.090	207
72.3	122.4	25.5	3.5	4		0.025	349
50.2	355.0	25.8	3	3.5	0.348	0.060	7
-39.0	80.7	25.9	2	2		0.018	69
1.5	190.9	26.2	3.5	3.5	0.311	0.029	177
-22.6	306.4	26.6	4	4	0.252	0.009	152
-20.3	275.3	26.7	8	8	0.208	0.045	239
3.7	52.3	26.9	6	7	0.158	0.044	227
37.8	41.7	27.0	4	5	0.317	0.026	253
-23.2	34.6	27.1	2.5	2.5	0.315	0.035	292
-11.4	218.4	27.7	3	3	0.261	0.059	201
15.0	54.3	27.9	3.5	5	0.204	0.033	265
34.6	119.9	28.0	8	8	0.261	0.019	233
60.3	286.5	28.4	3	3	0.281	0.068	55
19.1	290.4	28.8	2.5	2.5	0.334	0.041	9
25.2	133.6	29.1	7	7	0.233	0.016	251
-5.0	191.0	29.1	4	5		0.035	113
-63.4	53.0	29.5	8	8	0.260	0.041	140
52.6	326.5	29.6	4	6	0.211	0.042	282
-15.4	46.5	29.8	7	7	0.249	0.027	45
-23.0	300.4	29.9	2.5	4	0.271	0.033	164
6.3	141.8	30.2	2	2	0.249	0.034	242

TABLE 1 — *continued*

8.9	76.2	30.3	2	2.5	0.079	0.079	189
-25.9	143.9	30.4	3	3	0.301	0.004	25
41.7	122.6	31.0	1	2	0.367	0.071	190
20.3	331.8	31.1	4	4	0.291	0.014	126
-5.0	303.7	31.5	3.5	3.5	0.287	0.007	237
11.3	89.4	34.5	4	4	0.183	0.022	107
4.7	356.3	34.7	3	3	0.235	0.021	53
-59.9	178.9	35.6	3.5	3.5	0.206	0.022	82
14.7	194.0	36.2	2.5	3.5	0.240	0.028	168
-26.3	31.3	38.2	7	7	0.282	0.048	182
30.3	228.4	38.2	2	3	0.256	0.041	177
-45.7	174.8	38.6	3	3.5	0.235	0.042	203
0.8	5.3	39.1	3	3	0.314	0.045	205
-46.2	314.7	39.4	4	4	0.217	0.040	120
-42.0	271.9	42.5	7	7	0.316	0.036	170
-61.1	181.8	43.6	3.5	3.5	0.266	0.008	292
Additional craters plotted in Fig. 3							
-33.3	208.1	18.3	2	2	0.150		
10.4	171.4	19.5	3	4	0.302		
3.9	166.4	19.5	8	8	0.245		
-5.1	31.4	20.3	2	3.5	0.229		
-41.4	256.9	20.3	1	2	0.247		
9.3	26.9	20.5	2.5	3	0.259		
-5.7	349.6	21.8	3.5	3.5	0.217		
36.1	32.0	22.3	8	8	0.294		
47.7	14.9	23.6	3.5	4	0.188		
-23.6	190.6	29.6	3	3.5	0.381		
-22.6	137.2	29.6	8	8	0.249		
2.0	188.7	30.4	1	2	0.236		
44.1	201.5	31.4	1	3.5	0.278		
-32.2	314.9	37.5	3.5	3.5	0.232		
-43.5	101.7	38.7	4	4.5	0.104		
-24.2	344.1	38.8	1	4	0.323		
-39.4	37.7	42.4	3	3	0.214		
20.5	78.5	42.4	3	4	0.156		
8.6	298.8	44.0	3	3	0.392		
7.2	309.1	46.9	3.5	3.5	0.339		
-61.2	211.3	48.0	3	4	0.268		
45.3	146.3	48.0	3.5	4	0.305		
-24.6	296.1	48.4	4	4	0.240		
35.4	56.1	48.7	7	7	0.312		
-26.4	337.2	48.8	3	3	0.267		
-26.4	339.9	63.7	2.5	3.5	0.194		
-51.9	146.0	70.4	4	5	0.172		

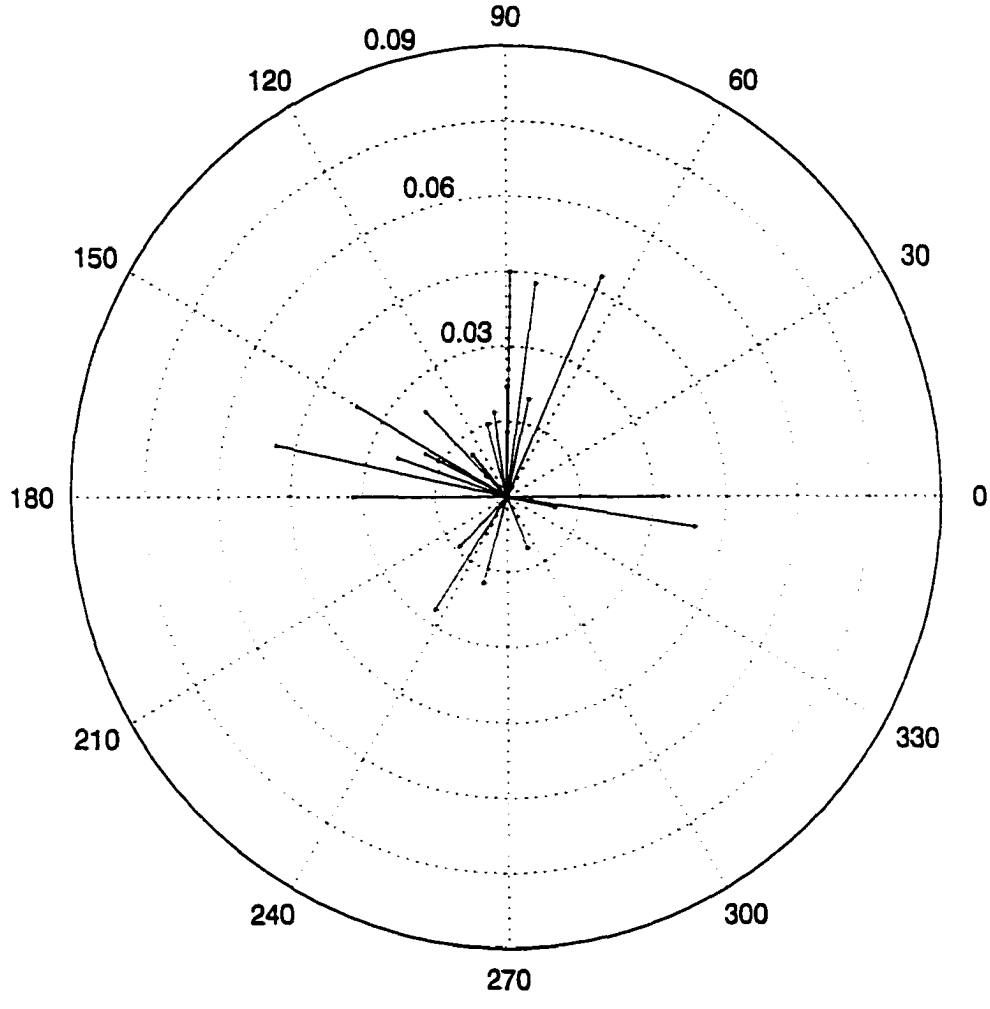

FIGURE 2: Central peak offsets for 25 high-angle impact craters. East is to the right. The average offset is 0.010 crater diameters at 116° (±0.003 east-west and north-south).

TABLE 2: Data for high-angle impact craters

Lat. (°N)	Long. (°E)	d	r	θ
-7.3	98.6	18.6	0.043	82
-44.2	86.8	18.8	0.005	352
-1.6	296.8	19.6	0.032	180
13.3	199.6	20.2	0.022	90
14.0	72.5	20.2	0.024	135
36.6	273.9	20.3	0.019	153
44.2	162.3	20.4	0.039	351
6.4	103.8	22.0	0.049	168
28.1	289.9	22.2	0.018	254
-12.3	287.6	22.6	0.024	161
44.9	11.5	23.3	0.014	225
28.3	72.7	23.3	0.048	66
-30.2	53.1	23.8	0.016	153
1.1	284.3	23.8	0.017	99
-52.8	127.2	24.2	0.006	136
23.0	81.3	25.1	0.013	90
-32.4	142.0	25.4	0.036	150
-58	13.6	25.5	0.020	77
80.9	223.3	26.5	0.045	89
16.5	109.4	27.0	0.010	348
-54.8	246.4	27.2	0.015	106
-75.9	277.6	27.3	0.011	292
78.4	174.7	29.8	0.027	236
-61.6	156.3	31.4	0.032	0
65.3	169.3	31.6	0.011	130

TABLE 2: Data for high-angle impact craters. d is the crater diameter in km, r the central peak offset magnitude as a fraction of the crater diameter, and θ the central peak offset angle in degrees counter-clockwise from the downrange direction.

expect to be able to use the uprange offset criterion collectively on groups of craters to tell whether they are oblique or not. However, such an attempt would also be futile, for two reasons: (1) in order to make a plot such as Fig. 1, one needs to know the direction of impact for each and every crater, and this is not known unless one already has access to other ways of determining obliquity, in which case the present method is of no use; (2) the average offset for high-angle impacts is so similar to that for oblique impacts that it is uncertain whether one can confidently distinguish the two groups based on average offset alone (a t-test on the data was only able to reject the null hypothesis that the average offsets are equal at a confidence level of 90%).

In Fig. 3, the normalized central peak diameters of 53 of the 60 craters in Fig. 1 plus an additional 27 oblique impact craters (listed in Table 1) are plotted against the impact angle class the crater was assigned to; 1 is steepest and 8 shallowest. The classification procedure is described in detail in the appendix. The upper axis shows the correspondence to impact angle found by correlating my classes with those given in Fig. 42 of Schultz (1992a). No correlation between central peak diameter and impact angle can be seen. The horizontal lines are not formal one-sigma error bars, but estimates of the range of possible classes. The average error in the central peak diameters is 0.018 crater diameters; in order not to clutter the graph any further, these error bars are not plotted.

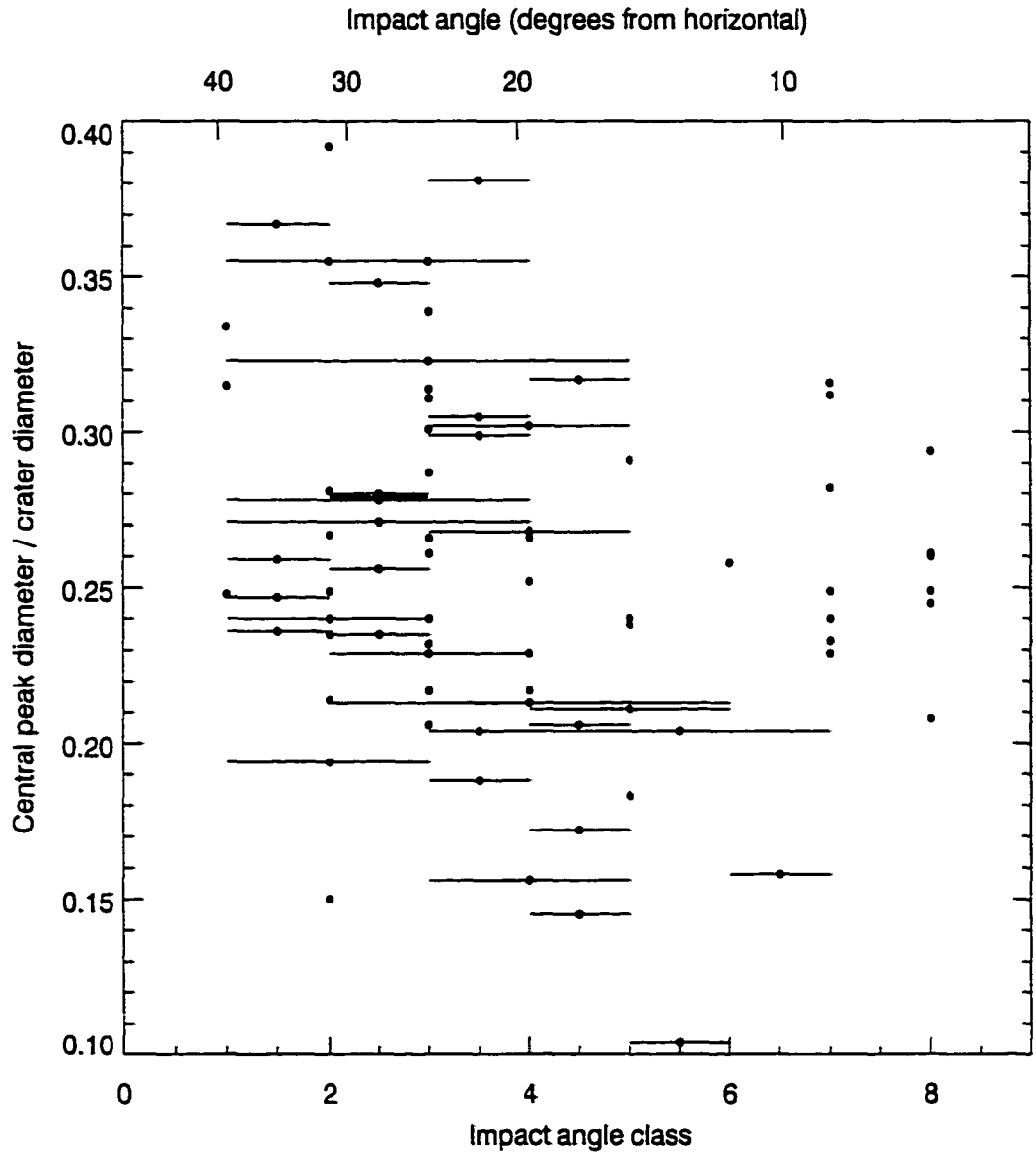

FIGURE 3: Normalized central peak diameters for 80 craters plotted against the impact angle class the crater was assigned to; 1 is steepest and 8 shallowest. The upper axis shows the correspondence to impact angles found by correlating my classes with those given in Fig. 42 of Schultz (1992a). The horizontal lines are not formal one-sigma error bars, but estimates of the range of possible classes.

CHAPTER 4

Discussion

4.1. Interpretation of the central peak offset data

Are the above results consistent with what we know about the formation of complex craters? It is believed that in oblique impacts, the deepest part of the transient cavity is offset uprange. For simple craters, this offset is preserved in the final crater, making the uprange wall steeper than the downrange wall (Gault and Wedekind, 1978; Forsberg et al., 1998). Schultz (1992b) argues that the offset is preserved also for complex craters, and that the central peak is centered on the deepest part of the crater (because central peaks form mainly from rebounding material from below the crater, and the rebound is centered on the deepest part of the transient cavity because that is the region of maximum compression). Therefore, the central peak in complex craters should be offset uprange. Schultz (1992a,b) argues that this is the case for most Venusian oblique impact craters.

As my results show, this conjecture is not supported by the data. Otherwise I agree that the central peak is probably centered on the deepest part of the crater, and that this is offset uprange in simple craters. However, the hypothesis that the region of maximum depth is offset uprange also in complex craters (resulting in an offset central peak) has no supporting evidence; any initial offset may well be eradicated by enhanced collapse of the steeper uprange wall of the transient cavity. A reasonable (but non-unique) interpretation of the data is that this is just what happens, and the observed offset distribution is simply a result of fluctuations in the exact amount of collapse.

4.2. The effect of possible interior volcanic flooding of craters

As mentioned in Chapter 2, my crater sample contains mostly dark-floored craters. Several authors have suggested that the floors of such craters have been flooded by lava subsequent to formation (e.g. Izenberg et al., 1994; Wichman, 1999; Herrick and Sharpton, 2000). In a crater where there are wall-slope asymmetries, flooding would displace the apparent center of the crater floor away from the steeper wall, towards the shallower wall. Because I (to correct for topography-induced distortions in the radar image) measured the range component of the central peak offset relative to the center of the crater floor, flooding of craters with wall-slope asymmetries in this direction would introduce further errors into my measurements. As wall-slope asymmetries in oblique impact craters would be expected to be aligned parallel with the impact direction, these errors would most likely affect the offset component along the uprange-downrange axis.

I am unfortunately unable to estimate the magnitude of these errors, as I do not know the magnitude of the potential slope asymmetries, but I can make some qualitative observations. If the asymmetry of the transient cavity is preserved in the final crater (something my results do not support), so that the uprange wall is steeper than the downrange wall, flooding would move the apparent central peak position uprange (ignoring possible central peak slope asymmetries, about which not much is known), and thus the "true" offset would be downrange of that measured. If the uprange wall is shallower than the downrange wall, the situation would be reversed. The former case strengthens, and the latter weakens, my conclusion that the central peaks in oblique

impact craters are not systematically offset uprange. If the asymmetries are random, there is no systematic effect.

When it comes to testing for a relationship between impact angle and central peak diameter, volcanic flooding of crater floors could have adverse effects in that it would increase the scatter of the measured central peak diameters over the scatter for the "true" diameters. This could in principle mask a relationship. However, because none of the craters in my sample are embayed from the outside, and as it is contentious in the Venus research community whether there has been any significant interior flooding of craters, I am reluctant to ascribe the scatter to this factor.

4.3. Applications

Are the above results applicable to any other planet but Venus? Most importantly, are they applicable to Earth, where the need for alternative methods to determine impact angles and/or directions is the greatest, as most craters have been eroded or buried so as to preclude the use of ejecta deposit shape and rim height variations? The factors that could affect central peak formation are gravity, the mechanical properties of the rock, and the presence of a medium above the surface, such as an atmosphere or an ocean. Unfortunately, there have been no studies done to ascertain the influence of these factors. I believe, however, that their influence is small, and since Earth is the planet most similar to Venus, terrestrial craters should be those most similar to Venusian craters.

Schultz and D'Hondt (1996) and Hildebrand et al. (1998) have used the observed offsets of the central gravity anomaly (assumed to correspond to the central uplift) of

Chicxulub crater to infer the direction of approach and impact angle of the Chicxulub bolide. In addition, Schultz and Anderson (1996) use both an offset central uplift and a large central uplift diameter relative to crater diameter to argue that the Manson impact structure in Iowa resulted from an oblique impact. I believe that the results presented in this thesis are cause for a re-evaluation of these arguments.

APPENDIX

Impact Angle Classification

My impact angle classification is based solely on the shape of the ejecta deposits. To first order, the shape is defined by the angle subtended by the uprange sector devoid of ejecta (the angle of avoidance). Table A.1 lists the eight classes and the corresponding angles of avoidance and impact angles. The impact angles were determined by correlating my classes with the ejecta deposit drawings (and associated angles) in Fig. 42 of Schultz (1992a).

For many craters the angle of avoidance was smaller close to the rim than farther away from it, or it was otherwise hard to decide what the angle really was. I therefore assigned to each crater a range of possible classes—this range is represented in Fig. 3 by the horizontal bars.

TABLE A.1: Impact Angle Classes

Impact angle class	Angle of avoidance	Impact angle
1	45°	40°
2	65°	30°
3	90°	25°
4	115°	20°
5	135°	15°
6	155°	12°
7	180°	9°
8	>180°	<6°

REFERENCES

Gault, D. E. and J. A. Wedekind, Experimental studies of oblique impact, *Proc. Lunar Planet. Sci. Conf. 9*, 3843–3875, 1978.

Gilbert, G. K., The Moon's face, a study of the origin of its features, *Bull. Philos. Soc. Wash. (D.C.) 12*, 241–292, 1893.

Ford, J. P., J. J. Plaut, C. M. Weitz, T. G. Farr, D. A. Senske, E. R. Stofan, G. Michaels, and T. J. Parker, *Guide to Magellan Image Interpretation*, JPL Publication 93-24, 1993.

Forsberg, N. K., R. R. Herrick, and B. Bussey, The effects of impact angle on the shape of lunar craters, *Lunar Planet. Sci. Conf. 29*, #1691, 1998.

Herrick, R. R. and N. K. Forsberg, The topography of oblique impact craters on Venus and the Moon, *Lunar Planet. Sci. Conf. 29*, #1525, 1998.

Herrick, R. R. and V. L. Sharpton, Implications from stereo-derived topography of Venusian impact craters, *J. Geophys. Res. 105*, 20,245–20,262, 2000.

Hildebrand, A. R., M. Pilkington, J. Halpenny, R. Cooper, M. Connors, C. Ortiz-Aleman, R. E. Chavez, J. Urrutia-Fucugauchi, E. Graniel-Castro, A. Camara-Zi, and R. T. Buffler, Mapping Chicxulub crater structure with overlapping gravity and seismic surveys, *Lunar Planet. Sci. Conf. 29*, #1821, 1998.

Izenberg, N. R., R. E. Arvidson, and R. J. Phillips, Impact crater degradation in Venusian plains, *Geophys. Res. Lett. 21*, 282–292, 1994.

Schultz, P. H., Atmospheric effects on ejecta emplacement and crater formation on Venus from Magellan, *J. Geophys. Res. 97*, 16,183–16,248, 1992a.

Schultz, P. H., Effect of impact angle on central peak/peak ring formation and crater collapse on Venus, in *LPI—Papers Presented to the International Colloquium on Venus*, 103–104, 1992b.

Schultz, P. H. and S. D'Hondt, Cretaceous-Tertiary (Chicxulub) impact angle and its consequences, *Geology 24*, 963–967, 1996.

Schultz, P. H. and R. R. Anderson, Asymmetry of the Manson impact structure: Evidence for impact angle and direction, in *The Manson Impact Structure, Iowa: Anatomy of an Impact Crater*, C. Koeberl and R. R. Anderson (eds.), Geological Society of America Special Paper 302, 397–417, 1996.

Shoemaker, E. M., Interpretation of lunar craters, in *Phys. and Astron. of the Moon*, Z. Kopal (ed.), Academic Press, N. Y., 283–359, 1962.

Wichman, R. W., Internal crater modification on Venus: Recognizing crater-centered volcanism by changes in floor morphometry and floor brightness, J. Geophys. Res. 104, 21,957–21,977, 1999.